coatings

Article

Wall Latex Paint with Graphene Oxide Incorporation

Jean Carlos Araujo Sousa [1], Rudnei José de Sousa [2], Bruna Pietroski de Lima [1], Luís Fernando Cusioli [3], Rúbia Carvalho Gomes Corrêa [1], Rosângela Bergamasco [3] and Natália Ueda Yamaguchi [1,*]

1 Post-Graduation Program in Clean Technologies, Cesumar Institute of Science, Technology and Innovation, Cesumar University, Maringá 87050-900, Brazil
2 Art Plus Revestimentos LTDA, Maringá 87065-310, Brazil
3 Chemical Engineering Department, Universidade Estadual de Maringá, Maringá 87020-900, Brazil
* Correspondence: natalia.yamaguchi@unicesumar.edu.br; Tel.: +55-44-30276360

Abstract: Graphene has stood out in several areas of research. The objective of the present work was an unprecedented study in the production of a commercial wall latex paint with graphene oxide incorporation. The developed paint was assessed by performance tests according to the Brazilian standards, and the characterization was performed using scanning electron microscopy (SEM), X-ray diffraction (XRD), Fourier-transform infrared (FTIR), thermogravimetric analysis (TGA), and contact angle analysis. The results indicated that GO addition led to a better dispersion of the paint compound mixture even at very low concentrations (1% and 2%). For the dry and wet paint coverage performance tests, the results were superior, 2% and 9%, respectively, when compared with the paint without GO addition. All performance tests were in accordance with the requirements of the Brazilian standards. Thus, it was concluded that GO-containing paint could be a promising building material to be used as a paint additive obtaining superior properties.

Keywords: acrylic paint; architectural coating; building paint; coating; nanomaterial; polymer

Citation: Araujo Sousa, J.C.; de Sousa, R.J.; de Lima, B.P.; Cusioli, L.F.; Gomes Corrêa, R.C.; Bergamasco, R.; Ueda Yamaguchi, N. Wall Latex Paint with Graphene Oxide Incorporation. *Coatings* **2022**, *12*, 1652. https://doi.org/10.3390/coatings12111652

Academic Editor: Gianfranco Carotenuto

Received: 29 September 2022
Accepted: 26 October 2022
Published: 31 October 2022

1. Introduction

The civil construction sector has a fundamental role in achieving the goals of sustainable development, since it is one of the sectors that consume the most natural resources and generate a large amount of waste. Sustainable construction consists of a system that promotes planning from a sustainable design and the execution and maintenance of the construction to guarantee its full functioning during its life cycle [1].

In the construction sector, the painting of buildings is a very important step, representing a significant cost in the overall budget. In addition to decoration, building painting has the functions of protecting, signaling, controlling the lighting of, and sanitizing the building, as well as influencing its thermal comfort [2].

Paints are defined as a fluid that can be spread onto a surface in a thin layer that forms a solid, cohesive, and adherent film. Generally, they consist of a binder, pigments, and solvent. In addition to these common components, there are several other elements, such as polymers, zeolites, bentonites, biocides, defoamers, surfactants, wetting agents, hydrophobic agents, dispersants, cosolvents, thickeners, coalescents, and extenders [3]. In the past, most paints were based on organic solvents, but because of environmental and health concerns, water-based coatings have been playing a more prominent role [4].

For the chemical industry, technological innovation is necessary. Wall paints elaborated with innovative technical procedures, techniques to improve their durability, and materials that minimize their environmental impact while providing more sustainable paints for civil construction result in an environment prepared for sustainable development [5].

Among the technologically innovative materials, graphene has stood out. Graphene is a single layer of carbon atoms, only one-atom thick in a two-dimensional hexagonal crystalline structure of carbon atoms linked by hybridized sp^2 bonds [6]. Due to its diverse properties, graphene has aroused enormous scientific interest in the production of various interesting and useful applications [7].

The myriad of exceptional properties of graphene opens up possibilities for many interesting types of paints and coatings. The high resistivity of graphene can produce durable coatings that do not crack and are resistant to water and oil; its excellent electrical and thermal conductivity can be used to make various conductive paints, and its strong barrier effect can contribute to antioxidant, antiscratch, resistant, anti-UV, and antibacterial paints. Graphene paints are gaining ground in the current market due to such properties and are already seen in graphic forms for printing, conductors for supercapacitors, and surface coatings, such as sprays and epoxy resins, among other applications [8–10].

The vast majority of applications found in previous literature use graphene as a coating. Thermal sensors, electrochemical sensors, solar cells, anticorrosive materials, and touch screens all require a coating, which encourages the development of graphene paints. Therefore, graphene has the possibility of being processed to produce functional paints, with varied rheological and morphological properties and different thicknesses, and printing processes and coatings, at low cost and with reliable industrial scale [8,9,11].

A number of challenges remain for the commercialization and industrialization of graphene. Regarding costs and production methods, new ultrafast, low-cost methods of mass and high-quality production are being developed [12] using carbon sources from waste, recycling, and upcycling [13]. As regards the price of graphene products, Lin et al. [14] state that it should be primarily determined by their performance and attractive properties, which satisfy specific application-dependent requirements and provide attractive benefits over other alternatives available in the market. In this way, ensuring the expansion of commercial material applications and realizing truly competitive applications, graphene can find its way to wide commercialization.

Thus, considering the great employability of graphene and its diverse properties, the present study proposed an unprecedented study of the development of a commercial wall latex paint with the incorporation of GO to improve its properties, aiming to produce a more sustainable paint with a greater yield, thereby reducing its consumption for domestic applications.

2. Materials and Methods

2.1. GO Synthesis

The synthesis of GO was performed using the modified Hummers method, as described in previous literature [15–17]. In summary, the methodology consisted of the oxidation of graphitic material to obtain graphite oxide, followed by exfoliation of the graphite oxide in water in an ultrasonic bath, resulting in a dispersed GO solution.

2.2. Preparation of Wall Latex Paint with GO Incorporation

A generic commercial formulation of a premium latex matt paint that meets the requirements of the Brazilian standards was provided by Art Plus Revestimentos Ltda. (Maringá-PR, Brazil). The wall paint formulation was developed on a bench scale using a reduction of 1:1000 L of the industrial scale. Thus, 1 L of paint was produced for each type of paint: one without the addition of GO, one with the addition of 1.0% GO, and a third one with 2.0% GO (m/m). The paints were produced in 2 L beakers using a mixer adapted with a bench drill (Motomil, Navegantes, Brazil, FBH-130i, 0.3 hp). After being prepared, the paints were stored in polypropylene bottles at room temperature until use for the characterization analysis and performance tests.

GO was added in the initial phase of the paint formulation in order to obtain a better mixture. The preparation of the GO solution was carried out by ultrasonication in distilled water in a digital ultrasound bath (Quimis, Diadema, Brazil, Q3350, 70W) for 96 h to completely exfoliate the GO in the water that was used in the production of the paint. The paint without GO was produced according to the same methodology, but without the addition of GO, to validate the comparison of the produced paints.

2.3. GO and Coatings Characterization

The characterization of the surface morphology of the as-synthesized GO was verified through SEM analysis in a Hitachi (Tokyo, Japan) TM3000 scanning electron microscope. The paints were used to coat a polycarbonate surface and dried for 1 week before being analyzed in a Shimadzu (Kyoto, Japan) SS-550 microscope. The structure and chemical composition of the GO and paints were evaluated by means of XRD in a Rigaku (Tokyo, Japan) MiniFlex 600 diffractometer, using a scanning speed of 0.5 degree/min and a range of 2θ from 5° to 80°. The functional groups in the GO and paint samples were analyzed by means of the FTIR analysis in a Varian 1000 spectrometer (Palo Alto, CA, USA, Scimitar series) with a 2 cm^{-1} resolution using KBr pellets at room temperature. Lastly, the wettability of the wall paints was determined by using static contact angle measuring equipment (Cam-Micro, Tantec, Lunderskov, Denmark) and was performed in triplicate, subjected to analysis of variance, and the means were compared by the Tukey test at a level of 5% probability using the Sisvar software (version 5.6, 2006, Federal University of Lavras, Lavras, Brazil) [18].

2.4. Application of Wall Latex Paints for Buildings

The wall latex paints developed were tested by following the Brazilian regulation conformity assessment requirements for civil construction paints [19]. Light-colored matt latex paints were chosen, and therefore, the minimum performance requirements for matt latex paint in light colors for buildings [20] were followed. The minimum requirements for commercializing matt latex paint for buildings are presented in Table 1. The experiments were carried out in triplicate, subjected to analysis of variance, and the means compared by the Tukey test at a level of 5% probability [18].

Table 1. Minimum requirements for matt latex paint for buildings according to the Brazilian standards [20].

Test	Unit	Performance Requirements	Reference
Dry paint film hiding power	m^2/L	≥6.0	[21]
Wet paint hiding power	%	≥90.0	[22]
Wet abrasion resistance with abrasive paste	cycles	≥100	[23]

3. Results and Discussion

3.1. GO and Coating Characterization

A noticeable color difference was observed in the films of wall paints coating with and without GO (Figure 1a), as the samples with GO showed darker colors due to the natural color of the GO, which is very dark (Figure 1b). This coloration was expected, and similar results for color were obtained in studies carried out by other authors [24–26], using paints with GO for other applications. This result is an indication that obtaining white paint would be more difficult, requiring more addition of titanium oxide, which could increase the cost of the product [27,28], due to the high cost of natural sources of white pigment and its production [28,29].

(a) (b) (c)

Figure 1. (**a**) Digital image of the coatings on a polycarbonate surface, (**b**) digital image of graphene oxide (GO) film, (**c**) SEM micrograph of GO film.

The surface characterization of GO was observed by SEM analysis (Figure 1c), and a characteristic morphology of this material can be noted. Numerous authors have reported similar results [30–32]. However, when observing the morphology of the coatings by SEM, their porous characteristics were noticed (Figure 2), which is characteristic of latex paints [33,34]. In the SEM image of the wall latex paint produced without GO (Figure 2a), the microstructure of the sample can be seen to consist mainly of randomly distributed individual particles with an average size of approximately 500 nm (inset Figure 2a) in clusters of varied sizes ranging from 1 to 5 µm. Similar results were found by Dragnevski and Donald [35], who also produced water-based latex paints. However, when comparing the coatings with and without the inclusion of GO by SEM analysis, GO nanosheets were observed acting like a wrapping (arrows in Figure 2b) of the paint components. This is an indication that the GO could have altered the properties of the paint with regard to the mixture of the compounds, as it can be observed in the inset in Figure 2b that the particles previously observed (inset in Figure 2a) were wrapped in graphene nanosheets. This could interfere with the resistance to abrasion and coverage power of the paint, in addition to its adhesion to a surface, as the formation of larger clusters of sizes in the range of 10 µm was also observed (Figure 2b).

Figure 3 presents the results of GO and latex paint with GO incorporation by XRD analysis. The results of the GO sample (Figure 3a) confirmed the successful synthesis of GO using the modified Hummers method by the presence of the strong diffraction peak at $2\theta = 9.5°$, which corresponds to the (0 0 1) plane [36]. However, this peak was not verified in the diffractograms of the paint with GO incorporation samples, which may be an indication that the concentrations of GO used were very diluted. Figure 3b shows the diffractogram of the paint with the addition of 2% GO, but all coatings presented practically the same XRD diffractograms. According to the XRD analysis, it was found that calcium was in the form of calcite ($CaCO_3$), and its crystalline peaks were observed at 2θ = 23.2, 29.2, 36, 39.5, 43.2, 47.5, 48.4, 57.5, 57.3, 59.6, 60.2, 63.2, and 64.2 [37,38]. Peaks of $CaCO_3$ were also found in XRD results of architectural paints containing graphene in a previous study [39]. This result also indicates that the addition of graphene facilitates the crystallization of calcium to form a more ordered arrangement as $CaCO_3$. In addition, $CaCO_3$ has an important influence on the properties of the architectural coating, as it acts as a main filler. Thus, the enhanced crystallinity of $CaCO_3$ is beneficial for improving water resistance and reducing water permeability [39]. Bentonite presented typical diffraction peaks of montmorillonite at $2\theta = 35.0°$, kaolinite at 20.2° and 25.2°, and quartz with diffraction peaks at 2θ = 22.2, 27.1, 48.5, and 54.4° [40,41]. Titanium was found as titania (TiO_2), with peaks at 2θ angles of 20.8, 27.5, 36.2, 39.5, 40.3, 44.1, 54.4, 56.7, 63.1, 68.2, and 69.3° [42,43].

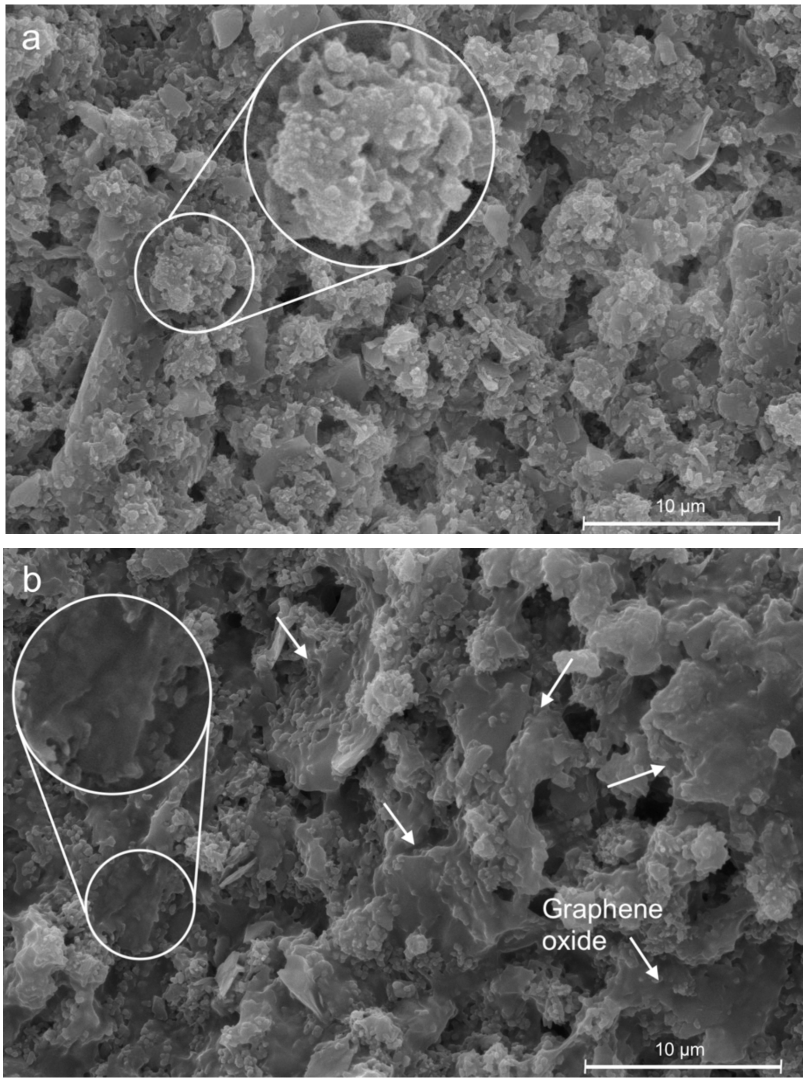

Figure 2. (**a**) SEM micrograph of the coating without the addition of graphene oxide (GO) and (**b**) SEM micrograph of the coating with 2.0% of GO incorporation.

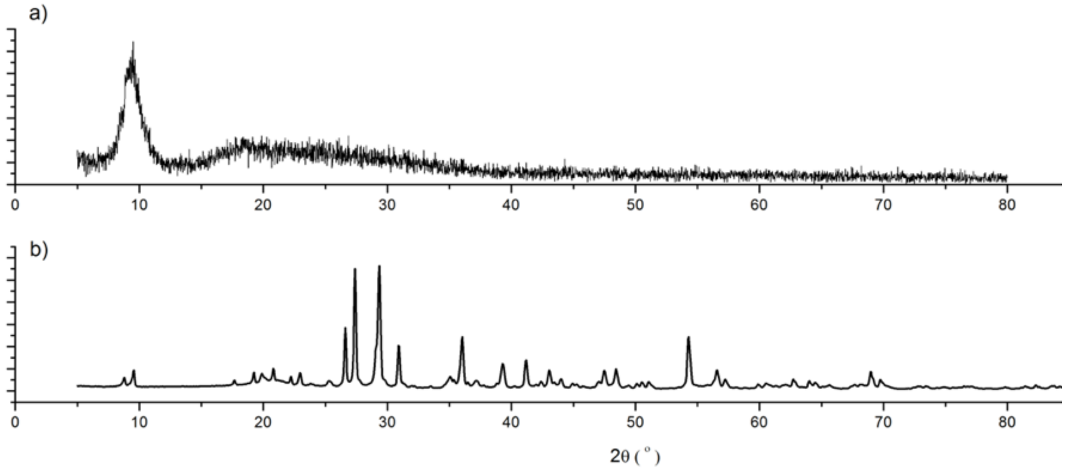

Figure 3. (**a**) XRD diffractogram of graphene oxide (GO) and of (**b**) wall latex paint with 2.0% of graphene oxide (GO) incorporation.

Figure 4 shows the GO spectra with characteristic absorption peaks at 3375 cm^{-1}, corresponding to the OH^- group; at 1719 cm^{-1}, indicating the possible occurrence of carboxyl groups (C = the corresponding to COOH groups); at 1625 cm^{-1}, which can be attributed to the aromatic bond C=C; at 969 and 828 cm^{-1}, which can be related to the epoxy group (vibrations of the C–O–C group); and at 1125 cm^{-1}, which can be attributed to the alkoxy group (C–OH) [44]. These results indicate that during the process of graphite oxidation with potassium permanganate and sulfuric acid by the modified Hummers method, parts of the structures that join the graphite layers were destroyed, and the functional groups with oxygen were inserted into its composition [15,45], proving again the successful synthesis of GO.

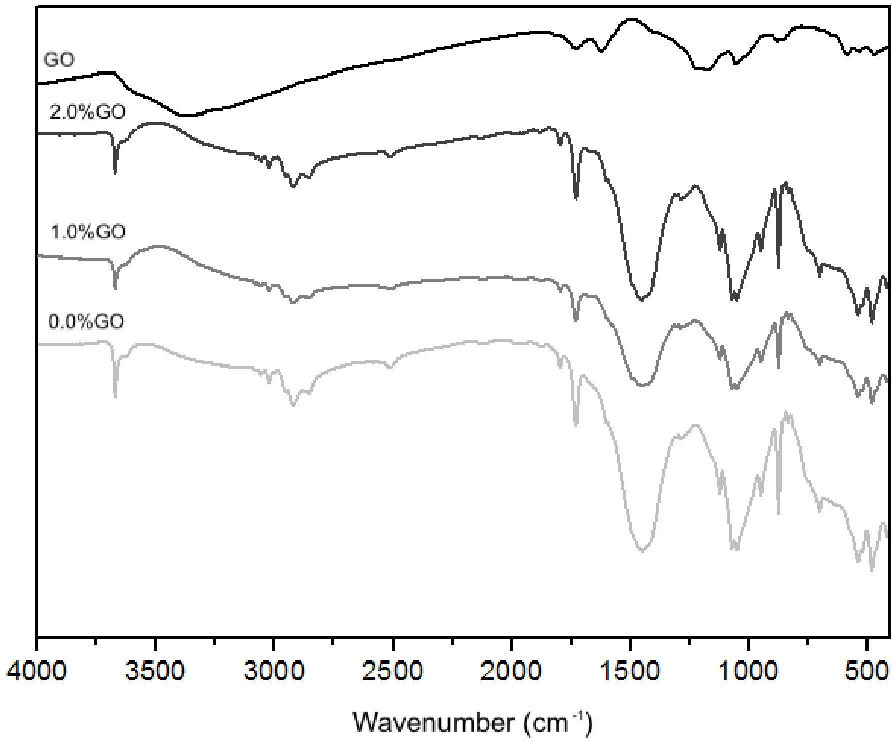

Figure 4. FTIR spectra of GO and wall latex paints with 0.0% of graphene oxide (GO), with 1.0% of GO and 2.0% of GO incorporation.

Figure 4 also shows the FTIR spectra of the developed paints, results used to characterize their chemical structures. Many common peaks expected for the binder, pigment, and filler were found in the paint. The peak observed at around 2900 cm^{-1} is due to the stretch band of C–H groups, while the peaks around 1725 and 1050 cm^{-1} correspond to the stretching vibrations C=O and C–OH, respectively. These peaks are all indicative of an acrylic binder material [42]. The absorption peaks around 1800, 1450, 850, and 700 cm^{-1} are characteristic of calcium carbonate, which is commonly used as a filler in the formulation of paints. Calcite, which is one of the most commonly found forms of calcium carbonate, presented peaks at 1450, 850, and 700 cm^{-1}. The peaks observed at 3700, 1100, and 925 cm^{-1} show the presence of hydrated aluminum silicate, which is also used as a filler in paint formulation. Quartz samples are also one of the mining forms of silica. For all studied samples, absorption peaks between 700 and 500 cm^{-1} are characteristic of TiO_2, since the strongest band belonging to TiO_2 was denoted in the region of 700–500 cm^{-1} by Colthup et al. [46]. In a study by Vitala et al. [47], bands between 600 and 450 cm^{-1} were assigned to amorphous TiO_2. Burgos and Langlet [48] studied the TiO_2 sol–gel reactions and, in IR studies, found bands belonging to the Ti-O and Ti-O-Ti groups in the 800–400 cm^{-1} range; therefore, the peaks at 475 and 550 cm^{-1} are related to the presence of TiO_2 in the paint samples produced. When comparing the FTIR spectra of the GO paint samples, it was not possible to identify the specific functional groups of GO in the new coatings. This may have occurred because of the small amount of GO used in comparison with the total sample volume, making it too diluted to be observed.

The thermograms present the results of the thermal analysis (Figure 5). The GO sample showed an initial loss of 15% up to 100 °C, which can be attributed to the loss of water that was adsorbed on the surface of the GO. Then, a further mass loss of 15% at 300 °C was observed resulting from the removal of oxygen-containing functional groups. The third, and greatest, mass loss at temperatures above 500 °C involves carbon pyrolysis [49,50]. For the paint samples, a similar behavior to that of graphene was observed, with loss of mass at 300 °C resulting from the removal of functional groups containing oxygen and a further loss of mass at temperatures of approximately 700 °C that involves the pyrolysis of the components present in paint. It was noted that the addition of GO contributed to a greater thermal degradation of the paint, since GO is more easily degraded in comparison with the materials present in the paint, such as bentonite, silica, and titanium oxide.

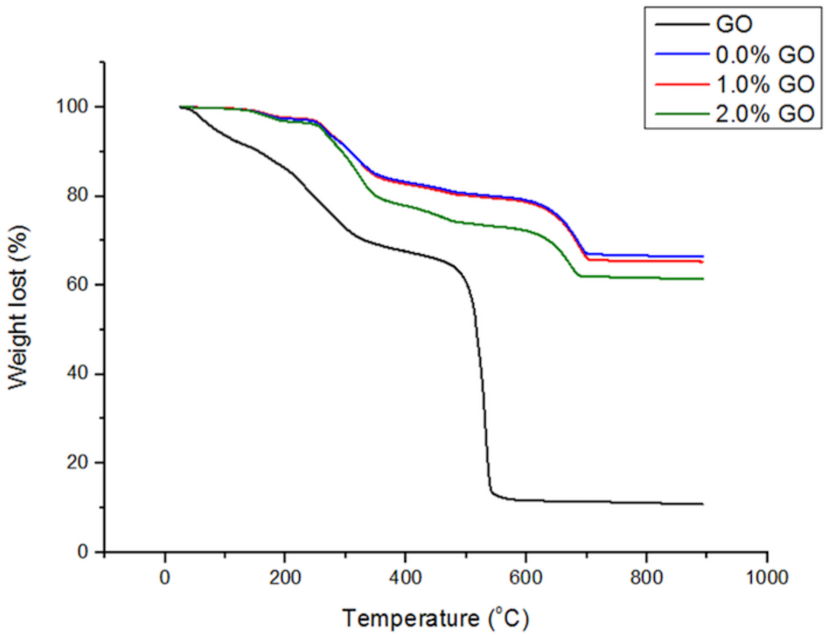

Figure 5. Thermograms of thermal analysis results for graphene oxide, wall latex paint without graphene oxide (GO), with GO 1.0%, and with GO 2.0% incorporation.

The static contact angle is an important analysis for coating characterizations [51]. The results for wettability of the building paints (Figure 6) demonstrate that all paints presented hydrophilic characteristics, as their static water contact angles were smaller than 90°. These results were expected as the latex paints are water-based paints, and waterborne coating films rarely exhibit contact angle with hydrophobic values [52].

The use of GO as additive increased the contact angle when using 1.0% of GO incorporation. However, for 2.0% of GO addition, the contact angle remained the same, with no significant difference from the control paint without GO addition. These results are very contradictory, as GO has been reported to provide an increase in hydrophilicity [53] and previous studies found that the contact angle of GO film is 29.5° [54], thus proving its hydrophilicity. However, roughness has been reported to also have a strong influence on the wettability of engineering surfaces [55]. Thus, low concentrations of GO may have increased the roughness of the surface and may have increased hydrophobicity with a more heterogeneous surface, but in higher concentrations, its hydrophilic characteristic may have resulted in the lowering of the contact angle. These results will directly affect the resistance and applicability of the building paints, as will be discussed in the conclusion. These results are in accordance with the SEM results (Figure 2) previously discussed.

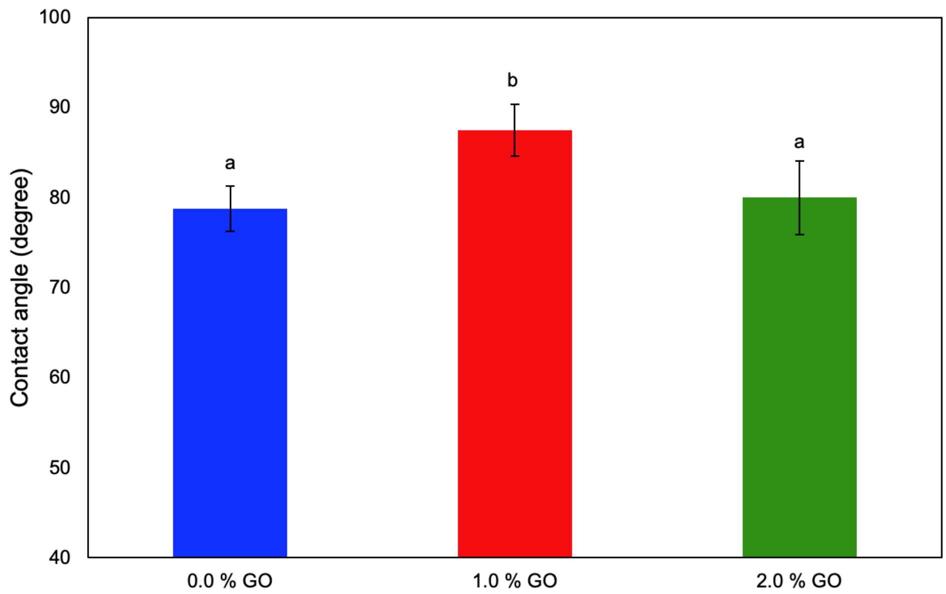

Figure 6. Static contact angles of water drop on the surface of wall latex paint without graphene oxide (GO), with 1.0% of GO, and with 2.0% of GO incorporation. The results marked with letter "a" do not differ statistically by Tukey test at a 5% of significance level.

Furthermore, paint with smaller contact angles becomes dirty more easily, and paint with larger contact angles is more likely to remain clean, as they are more hydrophilic and hydrophobic, respectively. Thus, the paint with 1.0% of GO addition, with a larger contact angle, will be least affected by moisture, which makes it more suitable for applications in humid environments [51].

3.2. *Application of Wall Latex Paints for Buildings*

The results obtained from the tests performed for the evaluation of the wall latex paint with and without the incorporation of GO are shown in Figure 7. All tests performed were in accordance to the minimum requirements of the Brazilian standards [20], and thus, the wall latex matt paint with GO addition could be used for both indoor and outdoor environments in civil construction sectors, such as for painting masonry surfaces in general in internal and external areas.

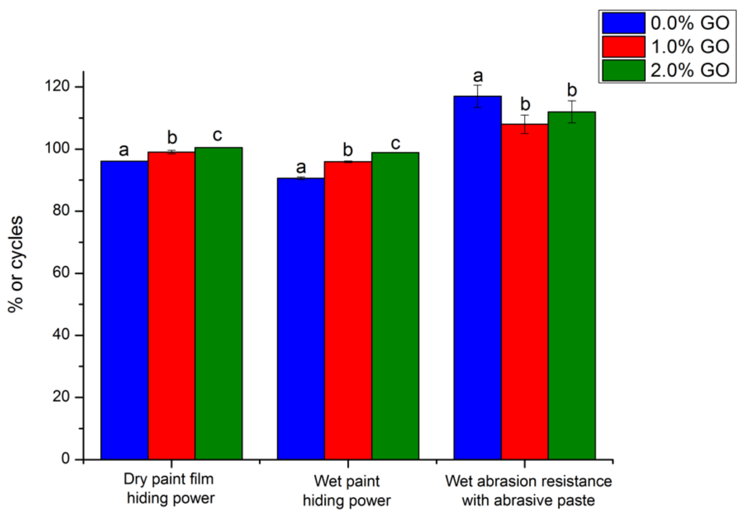

Figure 7. Evaluation results of wall latex matt paints developed with and without the incorporation of graphene oxide (GO). The results marked with the same letter do not differ statistically by Tukey test at a 5% of significance level.

The paints with GO increased the dry and wet hiding power in comparison with the paint without GO incorporation (0.0% GO). Furthermore, the concentration of GO also had an influence on hiding power, as the higher concentration presented better results. This result can be attributed to the larger clusters observed in the SEM analysis (Figure 2b) for the sample with GO incorporation. The larger clusters may have contributed to the better coverage and could be associated with a better mixture of the compounds added during the production of the paint.

The improvement in the coverage power of paints with GO addition indicates that GO as a paint additive contributes to produce more sustainable building paints in the construction sector, since its efficiency is higher in coverage power. This results in a reduction in paint consumption and, consequently, in the reduction of natural resources used and waste generated. It is also worth mentioning the benefit of the reduced amount of time needed for painting in civil construction, as with paint with GO addition, a higher paint yield is obtained and fewer layers of paint are needed, thereby increasing efficiency.

However, for resistance to wet abrasion, that is, the ability of a dry paint film to resist mechanical abrasion caused by brushing with an abrasive paste, the samples with GO presented lower resistance compared with the paint without GO. This result may be due to the hydrophilic characteristics of GO, which may have absorbed more water than samples without GO, thereby decreasing the abrasion resistance [56] as the test is carried out by washing and sanding [23]. Furthermore, the larger sizes of the clusters in the coating film may have also contributed to their easier removal in the abrasion test, as shown in the SEM micrographs in Figure 2, as previously discussed.

Table 2 presents some previous results of wall paints used for different applications. An incipient but promising field was observed, with many other possibilities of interesting and commercial applications.

Table 2. Wall paints with graphene as additive.

Paint	Application	Results	Reference
Water, pyrene, CaOH, and graphene quantum dot	Cultural heritage materials	Small 80 nm nanohybrids improved adhesivity, uniformity, anti-UV, and $CaCO_3$ formation.	[9]
Styrene-acrylic architectural coating and graphene	Electromagnetic interference (EMI) shielding	4% of graphene content improved dispersion stability, water and oxygen resistance, conductivity, and EMI shielding.	[39]
Trifluorovinyl chloride and vinyl ether copolymer and modified graphene oxide	Repair ancient architectural color paintings	Graphene oxide incorporation improved contact angle, water absorption, shear strength, light shielding performance, resistance to aging and salt.	[51]
Commercial water-based polyurethane paint with graphene nanoplatelets	Discrete strain and spatial sensing	The paint presented reduced adhesion and significant performance as discrete strain and spatial sensor.	[57]
Polydimethylsiloxane–graphene oxide modified waterborne polyurethane acrylate	Coatings painted on tunnels and highways	Improved thermal, mechanical, and hydrophobic properties.	[58]
Commercial premium latex matt paint and graphene oxide	Domestic application	1% of graphene oxide content improved mixture, hiding power, hydrophobicity, and $CaCO_3$ crystallization.	This study

4. Conclusions

A wall latex paint with GO incorporation was produced, and its performance as a paint for buildings was investigated according to the Brazilian standards. The characterization results confirmed the synthesis of GO by the modified Hummers method. The paints with and without the addition of GO were observed in SEM characterization analysis, and the results indicated that GO improved the dispersion and mixture of the compounds added during paint production and $CaCO_3$ crystallization. The results of the application of wall latex paints for buildings showed that the paint with GO incorporation presented better results for the dry and wet paint hiding power tests compared with the paint without graphene, and all tests performed were in accordance with the minimum requirements of the Brazilian standards. In addition, the paint with 1.0% of GO incorporation also presented better contact angle, suggesting that it had the best properties for hydrophobicity and cleanliness. Thus, the wall latex paint with GO incorporation has improved covering performance, with greater yield, and can be considered a more sustainable paint by reducing consumption and possibly also by requiring less cleaning. Further studies of paint rheology, color change, aging, water vapor permeability, stain resistance, surfactant lixiviation, and adhesion are recommended to better understand the novel material developed.

Author Contributions: Conceptualization, J.C.A.S. and N.U.Y.; data curation, J.C.A.S. and R.J.d.S.; formal analysis, N.U.Y.; investigation, J.C.A.S., L.F.C. and R.J.d.S.; methodology, J.C.A.S., L.F.C., R.J.d.S. and N.U.Y.; project administration, N.U.Y.; resources, N.U.Y. and R.B.; supervision, N.U.Y.; validation, N.U.Y.; visualization, N.U.Y. and J.C.A.S.; writing—original draft, J.C.A.S. and N.U.Y.; writing—review and editing, B.P.d.L., R.C.G.C. and N.U.Y. All authors have read and agreed to the published version of the manuscript.

Funding: This research was supported by Cesumar Institute of Science, Technology, and Innovation (ICETI/UNICESUMAR).

Institutional Review Board Statement: Not applicable.

Informed Consent Statement: Not applicable.

Data Availability Statement: The data presented in this study are available on request from the corresponding author.

Acknowledgments: The authors gratefully appreciate and acknowledge Art Plus Revestimentos Ltda. for the financial support, and for providing information and materials for the development of this study.

Conflicts of Interest: The authors declare no conflict of interest.

References

1. Fei, W.; Opoku, A.; Agyekum, K.; Oppon, J.A.; Ahmed, V.; Chen, C.; Lok, K.L. The Critical Role of the Construction Industry in Achieving the Sustainable Development Goals (SDGs): Delivering Projects for the Common Good. *Sustainability* **2021**, *13*, 9112. [CrossRef]
2. Mello, V.M.; Suarez, P.A.Z. As Formulações de Tintas Expressivas Através da História. *Rev. Virtual De Química* **2012**, *4*, 2–12.
3. Gupta, S.; Puttaiahgowda, Y.M.; Nagaraja, A.; Jalageri, M.D. Antimicrobial Polymeric Paints: An up-to-Date Review. *Polym. Adv. Technol.* **2021**, *32*, 4642–4662. [CrossRef]
4. Larson, R.G.; Van Dyk, A.K.; Chatterjee, T.; Ginzburg, V.V. Associative Thickeners for Waterborne Paints: Structure, Characterization, Rheology, and Modeling. *Prog. Polym. Sci.* **2022**, *129*, 101546. [CrossRef]
5. Van Timmeren, A.; Zwetsloot, J.; Brezet, H.; Silvester, S. Sustainable Urban Regeneration Based on Energy Balance. *Sustainability* **2012**, *4*, 1488–1509. [CrossRef]
6. Geim, A.K.; Novoselov, K.S. The Rise of Graphene. *Nat. Mater.* **2007**, *6*, 183–191. [CrossRef]
7. Han, M.; Muhammad, Y.; Wei, Y.; Zhu, Z.; Huang, J.; Li, J. A Review on the Development and Application of Graphene Based Materials for the Fabrication of Modified Asphalt and Cement. *Constr. Build. Mater.* **2021**, *285*, 122885. [CrossRef]
8. Bonaccorso, F.; Bartolotta, A.; Coleman, J.N.; Backes, C. 2D-Crystal-Based Functional Inks. *Adv. Mater.* **2016**, *28*, 6136–6166. [CrossRef]
9. Zhu, J.; Li, X.; Zhang, Y.; Wang, J.; Wei, B. Graphene-Enhanced Nanomaterials for Wall Painting Protection. *Adv. Funct. Mater.* **2018**, *28*, 1803872. [CrossRef]
10. Yu, J.; Lee, C.-H.; Kan, C.-W. Graphene Oxide/Reduced Graphene Oxide Enhanced Noniridescent Structural Colors Based on Silica Photonic Spray Paints with Improved Mechanical Robustness. *Nanomaterials* **2021**, *11*, 949. [CrossRef]
11. Sousa, J.C.A.; Santos, J.C.M.; Rubio, A.J.; Paccola, E.A.S.; Yamaguchi, N.U. Bibliometric Analysis of the Research Progress on Graphene Inks from 2008 to 2018. *Int. J. Chem. Mater. Eng.* **2019**, *13*, 308–312.

12. Sun, Z.; Hu, Y.H. Ultrafast, Low-Cost, and Mass Production of High-Quality Graphene. *Angew. Chem. Int. Ed.* **2020**, *59*, 9232–9234. [CrossRef]
13. Berktas, I.; Hezarkhani, M.; Haghighi Poudeh, L.; Saner Okan, B. Recent Developments in the Synthesis of Graphene and Graphene-like Structures from Waste Sources by Recycling and Upcycling Technologies: A Review. *Graphene Technol.* **2020**, *5*, 59–73. [CrossRef]
14. Lin, L.; Peng, H.; Liu, Z. Synthesis Challenges for Graphene Industry. *Nat. Mater.* **2019**, *18*, 520–524. [CrossRef]
15. Hummers, W.S.; Offeman, R.E. Preparation of Graphitic Oxide. *J. Am. Chem. Soc.* **1958**, *80*, 1339. [CrossRef]
16. Ferreira, M.E.C.; Soletti, L.d.S.; Bernardino, E.G.; Quesada, H.B.; Gasparotto, F.; Bergamasco, R.; Yamaguchi, N.U. Synergistic Mechanism of Photocatalysis and Photo-Fenton by Manganese Ferrite and Graphene Nanocomposite Supported on Wood Ash with Real Sunlight Irradiation. *Catalysts* **2022**, *12*, 745. [CrossRef]
17. Luciano, A.J.R.; Soletti, L.d.S.; Ferreira, M.E.C.; Cusioli, L.F.; de Andrade, M.B.; Bergamasco, R.; Yamaguchi, N.U. Manganese Ferrite Dispersed over Graphene Sand Composite for Methylene Blue Photocatalytic Degradation. *J. Environ. Chem. Eng.* **2020**, *8*, 104191. [CrossRef]
18. Ferreira, D.F. SISVAR: A computer analysis system to fixed effects split plot type designs: Sisvar. *Braz. J. Biom.* **2019**, *37*, 529–535. [CrossRef]
19. *Portaria nº529*; Requisitos de Avaliação da Conformidade para Tintas para Construção Civil. National Institute of Metrology Standardization and Industrial Quality: Brasília, Brazil, 2015.
20. *ABNT NBR 15079-1*; Paints for Buildings—Minimum Requirements for Performance. Part 1: Matte Latex Paint in Light Colors. Brazilian National Standards Organization: São Paulo, Brazil, 2011.
21. *ABNT NBR 14942*; Paints for Buildings—Method for Performance Evaluation of Paints for Non Industrial Buildings—Determinantion of Dry Paint Film Hiding Power and Theoretical Yield. Brazilian National Standards Organization: São Paulo, Brazil, 2016.
22. *ABNT NBR 14943*; Tintas Para Construção Civil—Método Para Avaliação de Desempenho de Tintas Para Edificações Não Industriais—Determinação Do Poder de Cobertura de Tinta Úmida. Brazilian National Standards Organization: São Paulo, Brazil, 2018.
23. *ABNT NBR 14940*; Tintas Para Construção Civil—Método Para Avaliação de Desempenho de Tintas Para Edificações Não Industriais—Determinação Da Resistência à Abrasão Úmida. Brazilian National Standards Organization: São Paulo, Brazil, 2018.
24. Giaveri, S.; Gronchi, P.; Barzoni, A. IPN Polysiloxane-Epoxy Resin for High Temperature Coatings: Structure Effects on Layer Performance after 450 °C Treatment. *Coatings* **2017**, *7*, 213. [CrossRef]
25. Singhbabu, Y.N.; Sivakumar, B.; Singh, J.K.; Bapari, H.; Pramanick, A.K.; Sahu, R.K. Efficient Anti-Corrosive Coating of Cold-Rolled Steel in a Seawater Environment Using an Oil-Based Graphene Oxide Ink. *Nanoscale* **2015**, *7*, 8035–8047. [CrossRef]
26. Tung, T.T.; Alotaibi, F.; Nine, M.J.; Silva, R.; Tran, D.N.H.; Janowska, I.; Losic, D. Engineering of Highly Conductive and Ultra-Thin Nitrogen-Doped Graphene Films by Combined Methods of Microwave Irradiation, Ultrasonic Spraying and Thermal Annealing. *Chem. Eng. J.* **2018**, *338*, 764–773. [CrossRef]
27. Gázquez, M.J.; Bolívar, J.P.; Garcia-Tenorio, R.; Vaca, F. A Review of the Production Cycle of Titanium Dioxide Pigment. *Mater. Sci. Appl.* **2014**, *5*, 441–458. [CrossRef]
28. Liang, Y.; Ding, H. Mineral-TiO2 Composites:Preparation and Application in Papermaking, Paints and Plastics. *J. Alloy. Compd.* **2020**, *844*, 156139. [CrossRef]
29. Razali, M.N.B.; Alkaf, A.A.; Zuhan, M.K.N.B.M. Formulation of Water-Based White Colour Paint from Waste Titanium Dioxide. *Mater. Today Proc.* **2022**, *48*, 1905–1909. [CrossRef]
30. Lima, A.M.; Faria, G.S.; Nardecchia, S.; Cruz, L.R.D.O.; Souza, M.D.M.V.M.; Pinheiro, W.A. Produção e caracterização de filmes finos transparentes e condutores de óxido de grafeno reduzido. *Matéria* **2017**, *22*, e11908. [CrossRef]
31. Rodbari, R.J.; Wendelbo, R.; Jamshidi, L.C.L.A.; Hernández, E.P.; Nascimento, L. Study of Physical and Chemical Characterization of Nanocomposite Polystyrene/Graphene Oxide High Acidity can be Applied in Thin Films. *J. Chil. Chem. Soc.* **2016**, *61*, 3120–3124. [CrossRef]
32. Su, H.; Li, Z.; Huo, Q.; Guan, J.; Kan, Q. Immobilization of Transition Metal (Fe^{2+}, Co^{2+}, VO^{2+} or Cu^{2+}) Schiff Base Complexes onto Graphene Oxide as Efficient and Recyclable Catalysts for Epoxidation of Styrene. *RSC Adv.* **2014**, *4*, 9990–9996. [CrossRef]
33. Dashtizadeh, A.; Abdouss, M.; Mahdavi, H.; Khorassani, M.; Hosseini, J. Modification and Improvement of Acrylic Emulsion Paints by Reducing Organic Raw Materials and Using Silica Nanocomposite. *J. Polym. Eng.* **2013**, *33*, 357–367. [CrossRef]
34. Cruz, C.G.; da Silveira, J.T.; Ferrari, F.M.; Costa, J.A.V.; da Rosa, A.P.C. The Use of Poly (3-Hydroxybutyrate), C-Phycocyanin, and Phenolic Compounds Extracted from Spirulina Sp. LEB 18 in Latex Paint Formulations. *Prog. Org. Coat.* **2019**, *135*, 100–104. [CrossRef]
35. Dragnevski, K.I.; Donald, A.M. An Environmental Scanning Electron Microscopy Examination of the Film Formation Mechanism of Novel Acrylic Latex. *Colloids Surf. A Physicochem. Eng. Asp.* **2008**, *317*, 551–556. [CrossRef]
36. Xiong, P.; Hu, C.; Fan, Y.; Zhang, W.; Zhu, J.; Wang, X. Ternary Manganese Ferrite/Graphene/Polyaniline Nanostructure with Enhanced Electrochemical Capacitance Performance. *J. Power Sources* **2014**, *266*, 384–392. [CrossRef]
37. Jeoung-Ah, K. The Characterisation of Paper Composite Porcelain in a Fired State by XRD and SEM. *J. Eur. Ceram. Soc.* **2004**, *24*, 3823–3831. [CrossRef]
38. Li, T.; Sui, F.; Li, F.; Cai, Y.; Jin, Z. Effects of Dry Grinding on the Structure and Granularity of Calcite and Its Polymorphic Transformation into Aragonite. *Powder Technol.* **2014**, *254*, 338–343. [CrossRef]

39. Li, Y.; Luo, J.; Huang, B.; Jin, H.; Sun, X.; Cao, C.; Chen, Q.; Qian, Q. Fabrication of Graphene-Modified Styrene–Acrylic Emulsion by In Situ Aqueous Polymerization. *Polymers* **2022**, *14*, 3763. [CrossRef]
40. Zhirong, L.; Uddin, M.A.; Zhanxue, S. FT-IR and XRD Analysis of Natural Na-Bentonite and Cu(II)-Loaded Na-Bentonite. *Spectrochim. Acta Part A Mol. Biomol. Spectrosc.* **2011**, *79*, 1013–1016. [CrossRef]
41. Cavalcanti, W.S.; Brito, G.D.F.; Agrawal, P.; Mélo, T.J.A.D.; Neves, G.D.A.; Dantas, M.M. Purificação e organofilização em escala piloto de argilas bentoníticas com tensoativo não iônico e aplicação em nanocompósitos poliméricos. *Polímeros* **2014**, *24*, 491–500. [CrossRef]
42. Topçuoğlu, Ö.; Altinkaya, S.A.; Balköse, D. Characterization of Waterborne Acrylic Based Paint Films and Measurement of Their Water Vapor Permeabilities. *Prog. Org. Coat.* **2006**, *56*, 269–278. [CrossRef]
43. Bao, Y.; Guo, R.; Ma, J. Hierarchical Flower-Like Hollow SiO_2@TiO_2 Spheres with Enhanced Thermal Insulation and Ultraviolet Resistance Performances for Building Coating. *ACS Appl. Mater. Interfaces* **2020**, *12*, 24250–24261. [CrossRef]
44. Beitollahi, H.; Hamzavi, M.; Torkzadeh-Mahani, M. Electrochemical Determination of Hydrochlorothiazide and Folic Acid in Real Samples Using a Modified Graphene Oxide Sheet Paste Electrode. *Mater. Sci. Eng. C* **2015**, *52*, 297–305. [CrossRef]
45. Lian, P.; Zhu, X.; Liang, S.; Li, Z.; Yang, W.; Wang, H. Large Reversible Capacity of High Quality Graphene Sheets as an Anode Material for Lithium-Ion Batteries. *Electrochim. Acta* **2010**, *55*, 3909–3914. [CrossRef]
46. Colthup, N.B.; Daly, L.H.; Wiberley, S.E. (Eds.) Copyright. In *Introduction to Infrared and Raman Spectroscopy*, 3rd ed.; Academic Press: San Diego, CA, USA, 1990; p. iv. ISBN 978-0-12-182554-6.
47. Viitala, R.I.; Langlet, M.; Simola, J.; Lindén, M.; Rosenholm, J.B. Aerosol–Gel Deposition of Doped Titania Thin Films. *Thin Solid Films* **2000**, *368*, 35–40. [CrossRef]
48. Burgos, M.; Langlet, M. The Sol-Gel Transformation of TIPT Coatings: A FTIR Study. *Thin Solid Films* **1999**, *349*, 19–23. [CrossRef]
49. Zhang, X.; Li, K.; Li, H.; Lu, J. Dipotassium Hydrogen Phosphate as Reducing Agent for the Efficient Reduction of Graphene Oxide Nanosheets. *J. Colloid Interface Sci.* **2013**, *409*, 1–7. [CrossRef] [PubMed]
50. Stankovich, S.; Dikin, D.A.; Piner, R.D.; Kohlhaas, K.A.; Kleinhammes, A.; Jia, Y.; Wu, Y.; Nguyen, S.T.; Ruoff, R.S. Synthesis of Graphene-Based Nanosheets via Chemical Reduction of Exfoliated Graphite Oxide. *Carbon* **2007**, *45*, 1558–1565. [CrossRef]
51. Fu, P.; Teri, G.-L.; Chao, X.-L.; Li, J.; Li, Y.-H.; Yang, H. Modified Graphene-FEVE Composite Coatings: Application in the Repair of Ancient Architectural Color Paintings. *Coatings* **2020**, *10*, 1162. [CrossRef]
52. Sbardella, F.; Pronti, L.; Santarelli, M.L.; Asua Gonzàlez, J.M.; Bracciale, M.P. Waterborne Acrylate-Based Hybrid Coatings with Enhanced Resistance Properties on Stone Surfaces. *Coatings* **2018**, *8*, 283. [CrossRef]
53. Choi, H.; Shah, A.A.; Nam, S.-E.; Park, Y.-I.; Park, H. Thin-Film Composite Membranes Comprising Ultrathin Hydrophilic Polydopamine Interlayer with Graphene Oxide for Forward Osmosis. *Desalination* **2019**, *449*, 41–49. [CrossRef]
54. Kim, J.; Khoh, W.-H.; Wee, B.-H.; Hong, J.-D. Fabrication of Flexible Reduced Graphene Oxide–TiO2 Freestanding Films for Supercapacitor Application. *RSC Adv.* **2015**, *5*, 9904–9911. [CrossRef]
55. Kubiak, K.J.; Wilson, M.C.T.; Mathia, T.G.; Carval, P. Wettability versus Roughness of Engineering Surfaces. *Wear* **2011**, *271*, 523–528. [CrossRef]
56. Saleiro, G.T.; Cardoso, S.L.; Toledo, R.; Holanda, J.N.F. Evaluation of the Crystalline Phases of Supported Titanium Dioxide in Red Ceramic. *Cerâmica* **2010**, *56*, 162–167. [CrossRef]
57. Tamburrano, A.; Proietti, A.; Fortunato, M.; Pesce, N.; Sarto, M.S. Exploring the Capabilities of a Piezoresistive Graphene-Loaded Waterborne Paint for Discrete Strain and Spatial Sensing. *Sensors* **2022**, *22*, 4241. [CrossRef]
58. Yang, J.; Li, J.; Muhammad, Y.; Yin, Y.; Meng, F.; Wei, Y.; Yang, H. Synthesis and Properties of Polydimethylsiloxane/Graphene Oxide Modified, Water-Based Polyurethane/Polyacrylate. *J. Appl. Polym. Sci.* **2019**, *136*, 47926. [CrossRef]